Podocyte Glutamatergic Signaling Contributes to the Function of the Glomerular Filtration Barrier

Laura Giardino,* Silvia Armelloni,* Alessandro Corbelli,*† Deborah Mattinzoli,* Cristina Zennaro,‡ Dominique Guerrot,§‖ Fabien Tourrel,¶ Masami Ikehata,* Min Li,* Silvia Berra,* Michele Carraro,** Piergiorgio Messa,*†† and Maria P. Rastaldi*

*Renal Research Laboratory and ††Department of Nephrology, Dialysis, and Renal Transplantation, Fondazione IRCCS Ospedale Maggiore Policlinico, Mangiagalli e Regina Elena and Fondazione D'Amico per la Ricerca sulle Malattie Renali, Milan, †MIA Consortium for Microscopy and Image Analysis, Monza, ‡Renal Child Foundation, G. Gaslini Children's Hospital, Genoa, and **University Department of Clinical and Experimental Medicine and Clinical and Experimental Neurosciences, University of Trieste, Trieste, Italy; and §Nephrology Department and ¶Department of Anaesthetics and Intensive Care, Rouen University Hospital, Rouen, and ‖INSERM UMR S 702, Paris, France

ABSTRACT

Podocytes possess the complete machinery for glutamatergic signaling, raising the possibility that neuron-like signaling contributes to glomerular function. To test this, we studied mice and cells lacking Rab3A, a small GTPase that regulates glutamate exocytosis. In addition, we blocked the glutamate ionotropic N-methyl-D-aspartate receptor (NMDAR) with specific antagonists. In mice, the absence of Rab3A and blockade of NMDAR both associated with an increased urinary albumin/creatinine ratio. In humans, NMDAR blockade, obtained by addition of ketamine to general anesthesia, also had an albuminuric effect. *In vitro*, Rab3A-null podocytes displayed a dysregulated release of glutamate with higher rates of spontaneous exocytosis, explained by a reduction in Rab3A effectors resulting in freedom of vesicles from the actin cytoskeleton. In addition, NMDAR antagonism led to profound cytoskeletal remodeling and redistribution of nephrin in cultured podocytes; the addition of the agonist NMDA reversed these changes. In summary, these results suggest that glutamatergic signaling driven by podocytes contributes to the integrity of the glomerular filtration barrier and that derangements in this signaling may lead to proteinuric renal diseases.

J Am Soc Nephrol 20: 1929–1940, 2009. doi: 10.1681/ASN.2008121286

It is widely recognized that most glomerular diseases are characterized by defects of the filtration barrier, where podocytes play a central role. Mutations of single podocyte proteins have been found at the basis of human nephrotic syndromes,[1] and podocyte deletion of the same molecules causes heavy proteinuria in experimental models.[2–8]

Podocytes are highly ramified cells: From the cell body depart a number of primary processes, further originating secondary foot processes. Starting from these features, it has been demonstrated that podocytes share numerous similarities with neurons: They both are terminally differentiated cells, have a common cytoskeletal organization, and have a common machinery of process formation.[9] Furthermore, a number of expression-restricted proteins, such as nephrin,[2] Neph1 and Neph2,[10] GLEPP1,[11] CAT3 and EAAT2,[12] synaptopodin,[13]

Received December 20, 2008. Accepted April 24, 2009.

Published online ahead of print. Publication date available at www.jasn.org.

Correspondence: Dr. Maria P. Rastaldi, Renal Research Laboratory, Fondazione IRCCS Policlinico and Fondazione D'Amico, Via Pace, 9-20122, Milan, Italy. Phone: 00390255033879; Fax: 00390248110814; E-mail: mp.rastaldi@fastwebnet.it

Copyright © 2009 by the American Society of Nephrology

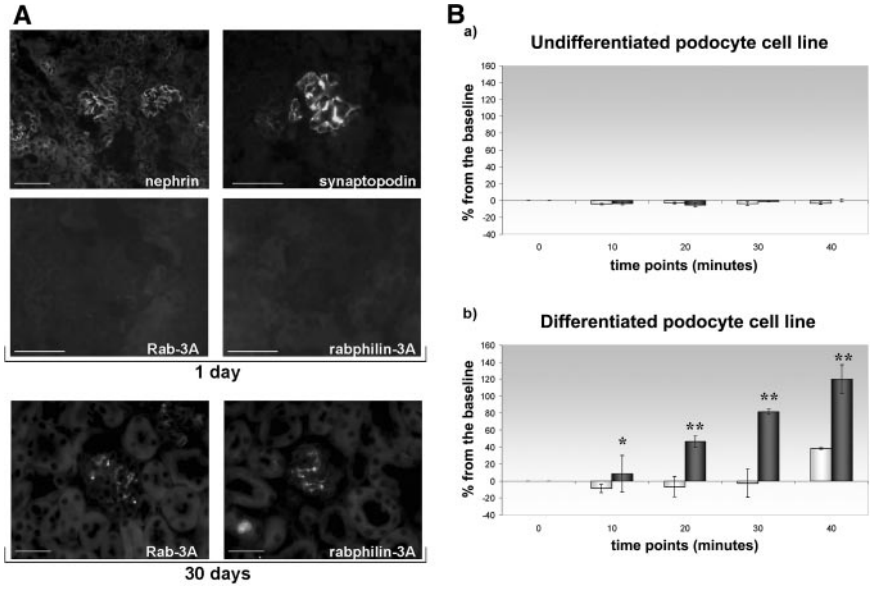

Figure 1. Glutamate exocytosis is a property of mature podocytes. (A) Developmental appearance of Rab3A and Rabphilin-3A. Compared with nephrin and synaptopodin, expressed in developing glomerular capillaries in newborn mice, Rab3A and rabphilin-3A stainings are completely negative (top, 1-d-old mouse). Both Rab3A and rabphilin-3A are positive in completely mature glomerular structures of a 30-d-old mouse (bottom). Indirect immunofluorescence: nephrin, bar = 100 μm; synaptopodin, Rab3A, and rabphilin-3A, bar = 50 μm; bottom, bar = 50 μm. (B) Glutamate exocytosis during podocyte differentiation. Glutamate was measured in the culture supernatant as expression of NADH generation at the beginning of the experiment (0) and every 10 min up to 40 min (time points on the *x* axis). Data come from three different sets of experiments, and results are expressed as percentage variation from the baseline (*y* axis, mean ± SD). (a) Spontaneous (□) and α-LTX–stimulated (■) glutamate exocytosis do not take place in undifferentiated podocytes grown at 33°C in presence of γ-IFN (see the Concise Methods section). (b) Differentiated podocytes display spontaneous (□) glutamate release at 40 min. Nanomolar α-LTX addition causes glutamate release at increasing concentrations (■). As it occurs in neuronal cells,[20,21] regulated exocytosis is greater than spontaneous glutamate release (*$P = 0.05$; **$P < 0.01$). Magnifications: ×200 in A, top, nephrin; ×630 in A, top, synaptopodin, Rab3A, and rabphilin-3A; ×400 in A, bottom.

drebrin,[14] and Sam68-like-MP2,[15] specifically belong to the podocyte and the neuron.

Our group has contributed to this line of research, initially by describing in podocytes the presence of Rab3A, a small GTPase that is mostly enriched in synaptic vesicles because it tightly modulates highly regulated exocytosis by acting through a number of effector molecules, including rabphilin-3a and Synapsin-I.[16] After finding that in podocytes, as it occurs in neurons, Rab3A associates to glutamate-containing vesicles along cell processes, we discovered that podocytes are equipped with a complete neuron-like glutamatergic signaling system.[17] We described that podocytes possess functional synaptic-like microvesicles and renal glomeruli express cognate glutamate transporters and receptors. These properties strengthened the analogies between podocytes and neurons and offered a rational interpretation to the biochemical similarity of foot process and synaptic adhesion complexes[17]; however, the role played by glutamate signaling in podocytes remained unanswered, and nothing was known about its relevance to podocyte and glomerular homeostasis. To get more details on the requirement of this neuron-like system of signaling by podocytes, we first conducted a preliminary analysis on its temporal appearance during podocyte differentiation. Then we studied conditions in which it was altered, on the vesicle and on the receptor side. The vesicular component was analyzed by studying the consequences of the absence of Rab3A. On the receptor side, we antagonized the ionotropic N-methyl-D-aspartate receptor (NMDAR), that we found present in human and rodent glomeruli, as well as in podocyte cell cultures.[17] Both Rab3A and NMDAR1 glomerular synthesis were also confirmed by *in situ* hybridization (Supplemental Figure 1) and by microarray expression data.[17]

RESULTS

Glutamate Release Is a Property of Mature Podocytes

We first looked at the expression of Rab3A, a marker of mature synapses,[18] and its effector rabphilin-3A in developing glomeruli of newborn mice. Different from other podocyte molecules, such as nephrin and synaptopodin, which are fully expressed by day 1 after birth, Rab3A and rabphilin-3A were still negative in developing glomeruli of 1-d-old mice and appeared subsequently, mainly by day 30, in mature glomeruli (Figure 1A), where podocyte location was confirmed by podocin co-labeling (Supplemental Figure 2).

These data suggested Rab3A and rabphilin-3A are part of a system needed by mature glomeruli; therefore, we analyzed glutamate release during podocyte differentiation by using a conditionally immortalized podocyte cell line,[19] derived from the *H-2K^b*-tsA58 transgenic mouse, in which the SV40 large T antigen is both temperature and γ-IFN dependent.

In neurons, spontaneous release typically occurs with a rate of one to two vesicles per minute per release site,[20] whereas evoked release occurs at a rate of >100 vesicles/s.[21] We evoked stimulated exocytosis by α-latrotoxin (α-LTX), a presynaptic neurotoxin widely used to trigger synaptic vesicles exocytosis.[22]

Undifferentiated podocytes, maintained at 33°C with γ-IFN, are proliferating cells that never exhibit a podocyte phenotype. In up to 40-min observation, these cells did not show

any glutamate release, either spontaneous or stimulated (Figure 1B, a).

By growing 15 d at 37°C without γ-IFN, cells stop to divide and differentiate to a mature podocyte phenotype. Their rate of spontaneous glutamate release was very mild and not measurable until 40 min. Addition of α-LTX elicited an outburst of glutamate, measurable at 10 min and progressively increasing (Figure 1B, b).

Rab3A-Knockout Model

Then we analyzed the possible appearance of a renal phenotype in Rab3A-null mice. Actually, Rab3A absence from podocytes became symptomatic by 3 mo of age, when Rab3A-knockout (KO) mice displayed macroalbuminuria (albuminuria/creatininuria ratio [U_{Alb}/U_{Creat}] = 302 ± 38 μg/mg; mean ± SD) that persisted over time, whereas lower values were detectable in wild-type (WT) mice (U_{Alb}/U_{Creat} = 157 ± 33 μg/mg; $P = 0.03$; Figure 2A).

KO and WT 3-mo-old kidneys did not show abnormalities by light microscopy (Figure 2B, a and b, e and f), whereas transmission electron microscopy demonstrated segmental areas of podocyte foot process effacement in KO glomeruli (Figure 2B, c; Supplemental Figure 3). By scanning electron microscopy, KO podocytes showed a disorganized, less ordered foot process structure (Figure 2B, d) than WT cells (Figure 2B, h). Focal and segmental decrease of podocyte proteins was detectable by immunofluorescence in KO glomeruli (Supplemental Figure 4, A through F) but was not accompanied by reduction of podocyte number (Supplemental Figure 4G). Overall, podocyte changes in Rab3A-KO mice offered a morphologic support to the evidence of macroalbuminuria; therefore, to understand the consequences of Rab3A absence in podocytes, we compared glutamate exocytosis in primary podocytes from Rab3A-WT and KO animals.

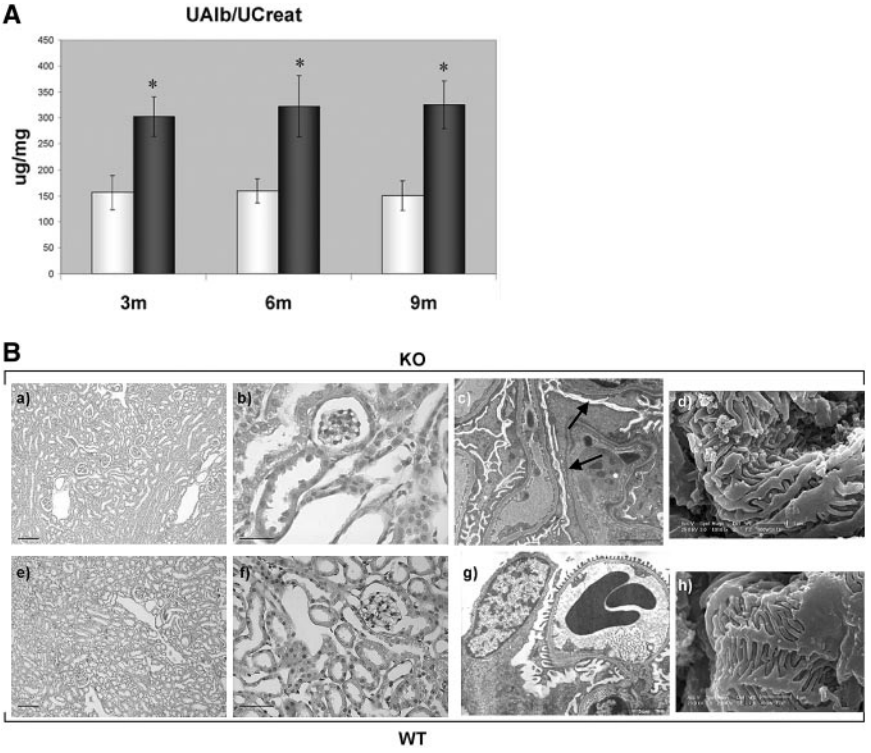

Figure 2. The renal phenotype of Rab3A-KO mice. (A) Macroalbuminuria is present in Rab3A-KO mice. U_{Alb}/U_{Creat} (μg/mg) was measured on 24-h urine samples in 27 Rab3A WT (□) and 27 KO animals (■). Data are means ± SD. Rab3A-WT (nine animals per age group, mean ± SD) show microalbuminuria, as expected according to the strain: 3m = 157 ± 33 μg/mg; 6m = 160 ± 23 μg/mg; 9m = 150 ± 29 μg/mg. Rab3A-KO (nine animals per age group, mean ± SD) display steady macroalbuminuria over time: 3m = 302 ± 38 μg/mg; 6m = 322 ± 59 μg/mg; 9m = 325 ± 46 μg/mg. *KO *versus* WT: $P = 0.03$. (B) Three-month-old Rab3A-KO and WT mice: Morphologic renal features. By light microscopy (KO: a and b; WT: e and f) kidneys display normal morphologic features (a and e: bars = 100 μm; b and f: bars = 50 μm). A glomerulus from a KO animal, observed by transmission electron microscopy (c; bar = 2 μm), shows segmental foot process effacement (arrows), whereas a glomerulus from a corresponding WT animal has normal foot processes (g; bar = 5 μm). Scanning electron microscopy allows the observation of disorganized podocyte foot process arrangement in a KO mouse (d; bar = 1 μm) and of the ordered structure of processes in a WT animal (h; bar = 1 μm). Magnifications: ×100 in B, a and e; ×400 in B, b and f; ×6000 in B, c and g; ×20000 in B, d and h.

A mild spontaneous release of glutamate from WT podocytes became detectable only after 40 min, and nanomolar concentrations of α-LTX (2.5 nM) caused a glutamate release measurable at 10 min and increasing with time (Figure 3A, a). Instead, KO podocytes demonstrated a spontaneous glutamate release already detectable at 10 min and gradually decreasing with time, but they did not show any response after α-LTX application (Figure 3A, b).

These results were confirmed by experiments in which recycling vesicles were monitored by the styryl dye FM1-43. Styryl dyes reversibly insert into the surface of lipid membranes and have no fluorescence properties in aqueous solution but become intensely fluorescent on membrane binding, allowing labeling of recycling vesicles that is detectable by fluorescence microscopy. In 20-min observation, WT podocytes did not become fluorescent when the dye was added alone, whereas a bright fluorescence signal appeared after α-LTX addition. Different from WT cells, KO podocytes became immediately fluorescent after addition of the dye, but the subsequent addition of α-LTX did not produce changes in cell fluorescence (Figure 3B).

To analyze further the different behavior of WT and KO podocytes, we studied the expression of Rab3A effectors rabphilin-3A and Synapsin-I. Rab3A exerts its role by switching

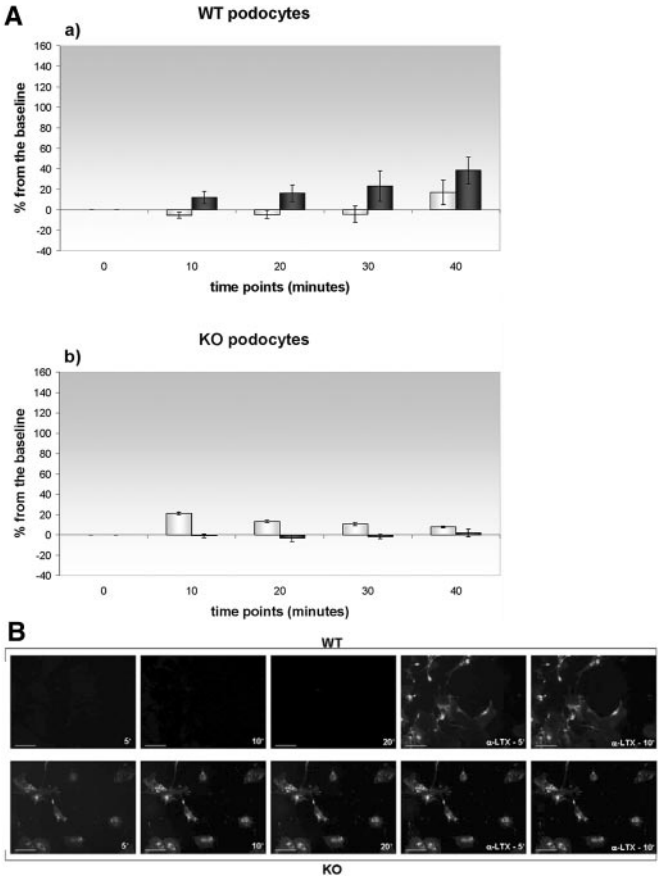

Figure 3. Differences in the pattern of glutamate exocytosis by WT and KO podocytes. (A) Glutamate exocytosis in primary podocytes from WT and KO mice. Glutamate was measured in the culture supernatant as expression of NADH generation at the beginning of the experiment (0) and every 10 min up to 40 min (time points on the *x* axis). Data come from three different sets of experiments, and results are expressed as percentage variation from the baseline (*y* axis, mean ± SD). (a) Spontaneous exocytosis in Rab3A-WT podocytes (□) is measurable at 40 min. Addition of α-LTX (■) produces glutamate exocytosis measurable at 10 min and increasing over time. (b) Rab3A-KO podocytes spontaneously demonstrate glutamate release (□) at 10 min but do not show any exocytosis when stimulated by α-LTX (■). (B) Vesicle recycling. WT and KO podocytes are loaded with the styryl dye FM1-43 at the beginning of the experiment, and vesicle recycling is followed by live microscopy. WT cells (top) do not take up the dye in 20-min observation. After addition of α-LTX, cells become and remain fluorescent. The dye instead spontaneously inserts on the membrane of KO cells (bottom), and fluorescence does not change with the addition of α-LTX. Bars = 100 μm. Magnification, ×200.

between a GDP-cytosolic form to a GTP vesicle–linked form, which interacts with multiple effectors. When GTP-Rab3A recruits rabphilin-3A and Synapsin-I, they control vesicle motility by regulating vesicle-actin association. Rabphilin-3A accomplishes this task by interacting with α-actinin,[23] and Synapsin-I acts by switching between a phosphorylated and a dephosphorylated form, respectively releasing or anchoring vesicles to actin.[24]

Compared with WT cells, Rab3A-KO podocytes displayed decreased expression of both effectors (Figure 4, A through C), but despite total Synapsin-I reduction, KO podocytes had more phosphorylated Synapsin-I than WT cells (Figure 4D).

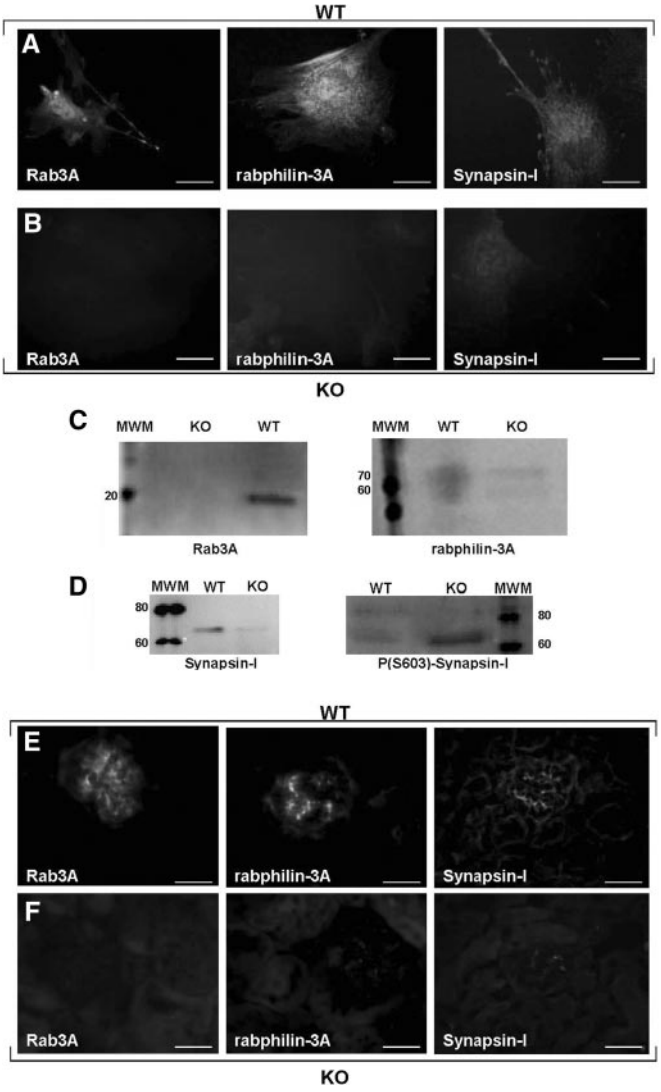

Figure 4. Rab3A effector molecules. (A through D) Rab3A effector molecules in cultured podocytes. Compared with WT cells (A), that along Rab3A express rabphilin-3A and Synapsin-I, KO podocytes (B) look negative for Rab3A and show a decreased expression of both the effectors rabphilin-3A and Synapsin-I. Indirect immunofluorescence, bars = 50 μm. (C and D) Western Blot analysis confirms the presence of Rab3A only in WT podocytes and the reduction of rabphilin-3A and Synapsin-I in KO podocytes. (D) Phosphorylated Synapsin-I is instead lower in WT than in KO cells. (E and F) Rab3A effector molecules in mouse glomeruli. WT glomeruli (E) express Rab3A and its effectors, whereas the absence of Rab3A in a KO mouse (F) is accompanied by reduced expression of rabphilin-3A and Synapsin-I. Indirect immunofluorescence, bars = 50 μm. Magnification, ×400.

Rabphilin-3A and Synapsin-I downregulation were confirmed by immunofluorescence in KO glomeruli (Figure 4, E and F), and higher expression of phospho-Synapsin-I was confirmed in KO animals by immunogold electron microscopy (Supplemental Figure 5).

NMDAR Blockade as a Model of Receptor Alteration

To block the NMDAR, we alternatively used norketamine hydrochloride or dizocilpine maleate (MK-801), which are selective, noncompetitive antagonists that act by binding to the phencyclidine binding site located within the ion channel, thereby preventing Ca^{2+} flux. We first applied the antagonists on cultured cells, namely primary podocytes from Balb/c mice and the differentiated podocyte cell line.

Either norketamine or MK-801, applied for 30 min at the concentration of 50 and 10 μM, respectively, was sufficient to cause a profound remodeling of podocyte cytoskeleton, as evidenced by almost complete disappearance of actin stress fibers and myosin-IIA redistribution (Figure 5A, a, b, d, and e). These changes were accompanied by disappearance of nephrin from podocyte processes (Figure 5A, g and h) and, similar to neuronal cells,[25] by an increased expression of NMDAR1 (Figure 5B). We were able almost to completely reverse cytoskeletal remodeling and nephrin redistribution when incubation with norketamine was followed by addition of the agonist NMDA, applied at a concentration of 50 μM for 15 min (Figure 5A, c, f, and i).

NMDAR is a calcium channel tightly linked to the actin cytoskeleton. At the synapse, NMDAR activation leads to intracellular calcium rise that activates calmodulin-dependent protein kinase II (CaMKII) by phosphorylation. In turn, phospho-CaMKII phosphorylates a series of downstream mole-

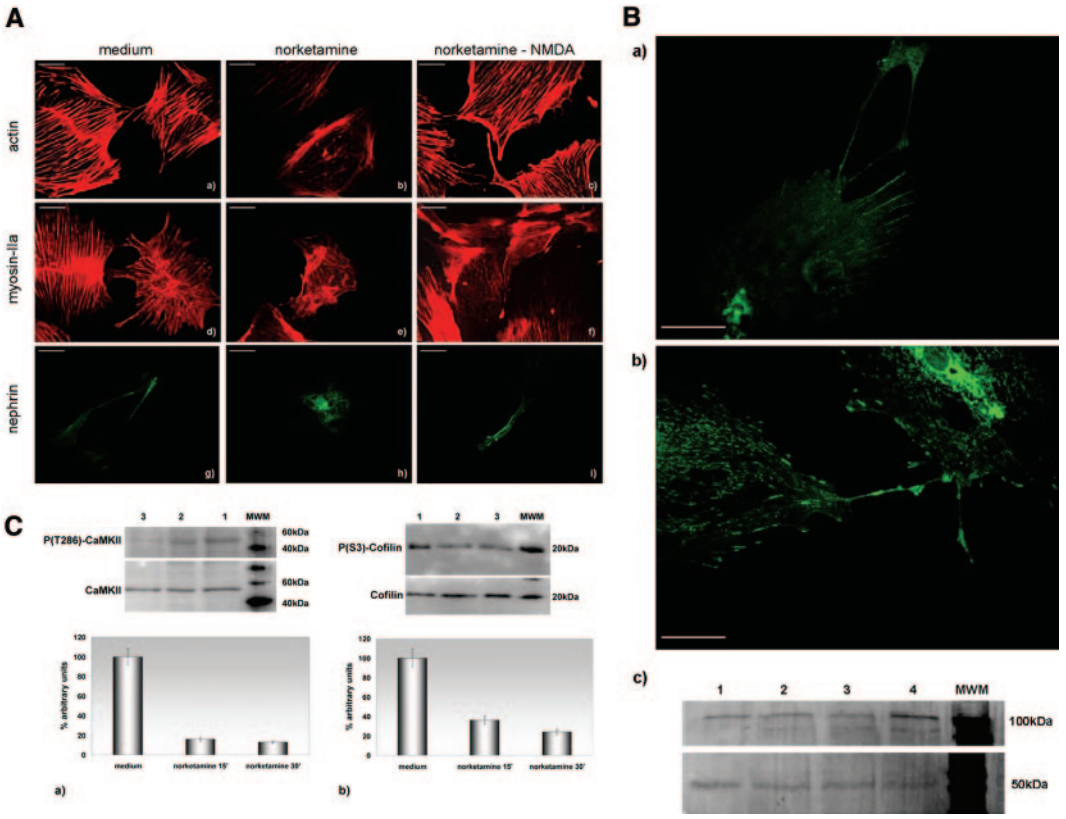

Figure 5. NMDAR *in vitro* blockade. (A) Effects on the cytoskeleton and nephrin expression. (a, b, d, e, g, and h) Compared with cells incubated with medium (a, d, and g), application of the NMDAR antagonist norketamine hydrochloride produces remodeling of the actin (b) and myosin IIA (e) cytoskeleton and redistribution of nephrin (h), which disappears from cell processes. (c, f, and i) The addition, after the antagonist, of the agonist NMDA, abolishes almost completely the agonist's effects. Phalloidin-TRITC (a through c); indirect immunofluorescence (d through i); bars = 50 μm. (B) Effects on NMDAR1 expression. (a and b) Compared with cells incubated with medium (a), addition of norketamine hydrochloride (b) determines an increased expression of the NMDAR1. Indirect immunofluorescence, bars = 50 μm. (c) Cells incubated with medium (lanes 1 through 3) express less NMDAR1 (band of approximately 100 kD) than cells treated by norketamine hydrochloride (lane 4). The lower band of 50 kD represents tubulin (loading control). (C) Downstream effects of the NMDAR blockade. Compared with cells incubated with medium (a and b, lane 1), phosphorylated CaMKII (a) and phosphorylated cofilin (b) are reduced, as compared with total CaMKII and total cofilin, after 15 (lane 2) and 30 min (lane 3) of treatment with norketamine hydrochloride. The graphs show a densitometric representation of Western blot results obtained from three experiments, where the ratio of lane 1 is taken at the arbitrary value of 100. Magnification, ×400.

cules, including cofilin, thereby regulating actin dynamics.[26] Western blot analysis of CaMKII and cofilin in cultured podocytes, after 15 and 30 min of incubation with the NMDAR antagonist, showed at both time points a reduced CaMKII phosphorylation and reduced phosphorylation of cofilin (Figure 5C), likely responsible for actin remodeling.

To establish whether the NMDAR blockade had a direct effect on glomerular permeability, we measured differences in convective glomerular albumin permeability (PAlb) on isolated rat glomeruli incubated with either norketamine or MK801 at various concentrations and time points. Both antagonists, particularly at the same concentrations and times used on cultured cells, were able to increase significantly glomerular PAlb (Figure 6, A through C). The effect of norketamine was completely reversed when glomeruli were subsequently incubated with NMDA (50 μM for 15 min), whereas only a mild effect was achieved when NMDA followed the more potent MK-801 (Figure 6D); therefore, we moved to the *in vivo* approach, by intraperitoneal norketamine injection in 16 Balb/c mice for 3 d at the concentration of 0.3 mg/100 g, which is at least 20 times less than the anesthetic dosage[27] and one 10th the concentration required to induce psychotic symptoms in rodents.[28] Sixteen control mice were administered an injection of saline.

U_{Alb}/U_{Creat}, evaluated on 24-h urine, increased after norketamine treatment (Figure 7A). Histology did not show major glomerular alterations; however, immunofluorescence demonstrated a globally decreased expression of nephrin (Figure 7B) in treated animals.

Norketamine hydrochloride is the major metabolite of ketamine, a general anesthetic optionally included in many routine protocols. A prospective pilot study was conducted to verify whether also in humans its application could be related to U_{Alb}/U_{Creat} differences. According to the inclusion criteria (see the Concise Methods section), 43 patients were initially enrolled. Three patients were excluded because of per-procedure hemodynamic instability. A final cohort of 40 patients was analyzed. Ketamine+ and ketamine− groups were comparable in terms of age, body mass index, estimated GFR, baseline U_{Alb}/U_{Creat}, and mean arterial pressure at H0 (before anesthesia) and H1 (1 h after anesthesia; Table 1). Percentage of celioscopic surgery (68% in ketamine+ *versus* 71% in ketamine−; $P = 0.89$), use of isoflurane for anesthesia maintenance (33 *versus* 29%; $P = 0.99$), and aminoglycosides (13 *versus* 12%; $P = 0.89$) were comparable as well. Although not reaching statistical significance ($P < 0.16$), ketamine+ subjects had higher H1/H0 of U_{Alb}/U_{Creat} than ketamine−, with a median multiplication factor in U_{Alb}/U_{Creat} between H0 and H1 of 9.0 (4.3 to 15.6) in ketamine+ and 4.2 (2.7 to 8.8) in ketamine− (Figure 8).

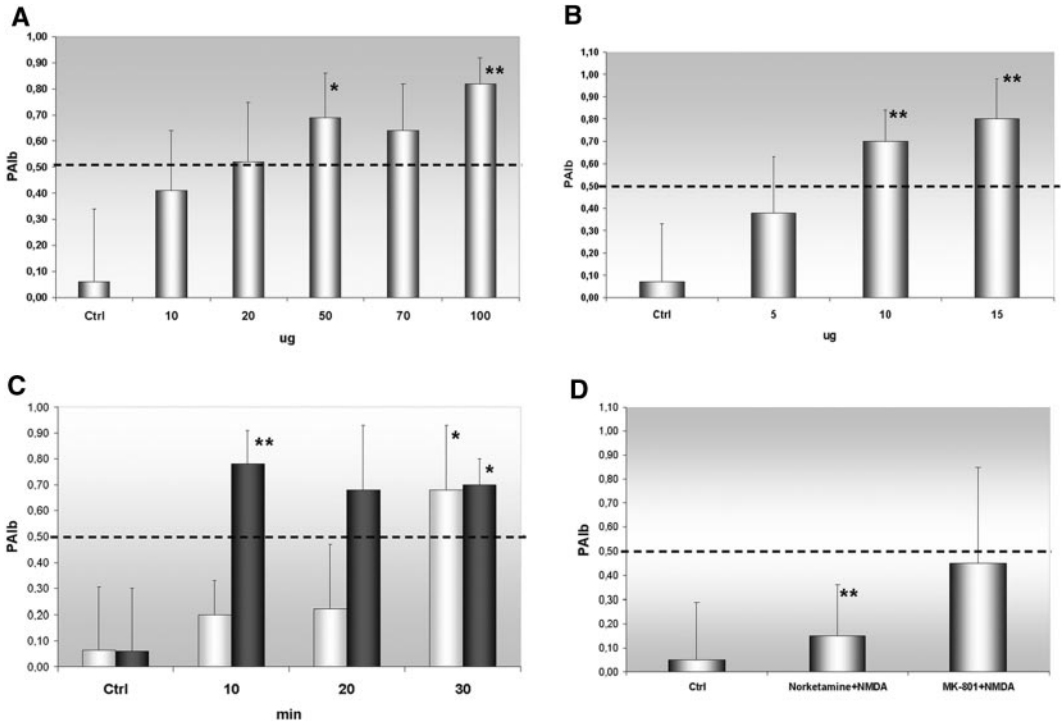

Figure 6. (A and B) Effects of NMDAR blockade on PAlb. Application of growing dosages of norketamine hydrochloride (A) and MK-801 (B) on isolated glomeruli (see the Concise Methods section) has a dosage-dependent effect on PAlb, compared with the application of medium alone (Ctrl). (C) The same concentrations used in the *in vitro* experiments produce effects at different times: 50 μM norketamine (□) changes PAlb when applied for at least 30 min, whereas 10 μM of the more potent MK-801 (■) becomes effective already after 10 min. (D) The addition of the antagonist NMDA at a dosage of 50 μM, and applied for 15 min, completely abolishes norketamine effects, whereas it only mildly reduces the action of MK-801. *$P < 0.005$ *versus* Ctrl; **$P < 0.001$ *versus* Ctrl.

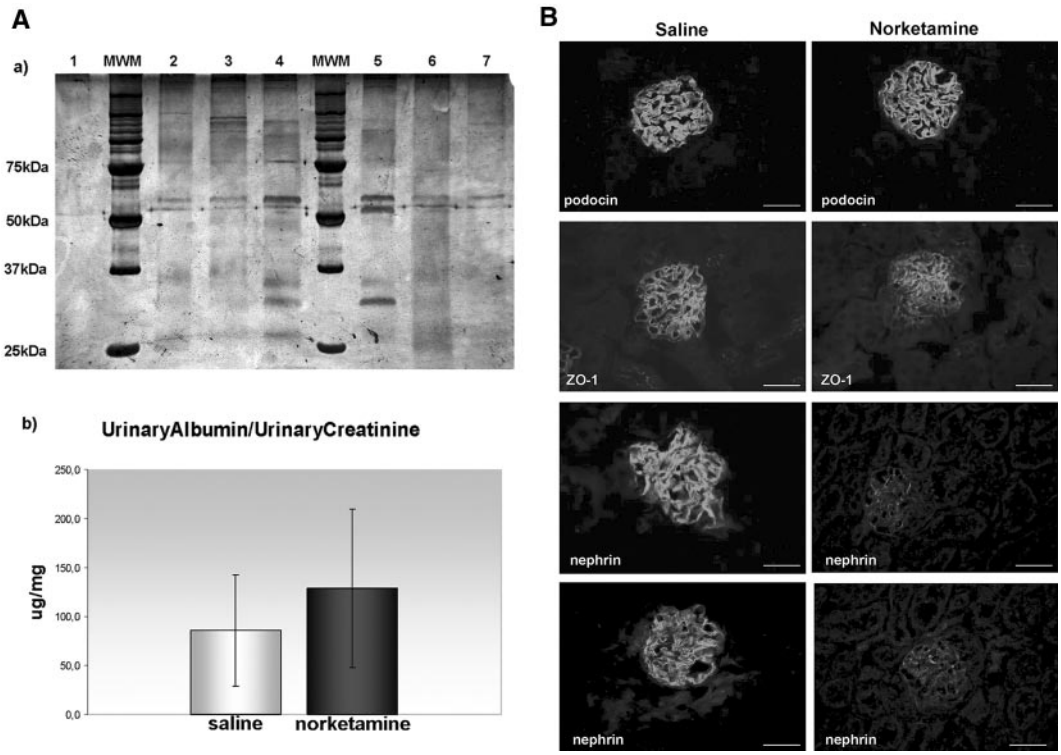

Figure 7. NMDAR *in vivo* blockade. (A) Measurement of albuminuria. (a) Representative results from 3-mo-old animals, intraperitoneally injected with either saline (lanes 2, 3, 6, and 7) or norketamine hydrochloride (lanes 4 and 5) for 3 d. Twenty-four-hour urine samples were collected, run on an SDS-PAGE, and silver stained. Albumin bands (molecular weight approximately 60 kD) are increased, and other bands of lower molecular weight appear in the urine of norketamine-injected animals (lanes 4 and 5). Lane 1 is a negative control, made by running PBS alone. (b) U_{Alb}/U_{Creat} from urine samples of all animals (mean ± SD). Although not statistically significant, mean U_{Alb}/U_{Creat} is higher in the group injected with norketamine, compared with saline-injected controls. (B) Evaluation of podocyte-specific proteins. Comparison of podocyte proteins in glomeruli from a saline-injected (left) and a norketamine-injected (right) mouse. Podocin staining is identical in both samples, whereas a segmental reduction of ZO-1 and a global decrease of nephrin can be noticed in glomeruli of the norketamine-treated mouse, as compared with the staining of the saline-injected animal. Indirect immunofluorescence, bars = 50 μm. Magnification, ×400.

DISCUSSION

Glutamate is the major excitatory neurotransmitter in the central nervous system, and its signaling at synapses has been extensively studied.[29] Meanwhile, evidence gathered during the past decade has shown the existence of functional glutamate signaling in several non-neuronal cells, such as osteoblasts,[30] pancreatic β islet cells,[31] and megakaryocytes.[32] We previously observed that podocytes are equipped with the necessary vesicular and receptor apparatus to use glutamatergic transmission,[17] and here we show that glutamatergic signaling driven by podocytes seems relevant to the maintenance of glomerular filter integrity, because its dysregulation is accompanied by podocyte alterations and increased albuminuria.

The question arising is why cells other than neurons would use glutamate for signaling. As for the glomerulus, we know that the entire blood volume passes the filter every 5 to 6 min, meaning that the glomerular barrier is constantly exposed to continuous physical (BP) and chemical (blood content) microenvironmental changes; therefore, effectiveness in maintaining filter homeostasis highly depends on efficient intercellular communication. Glutamate perfectly fits the need because, different from other types of intercellular communication, it has the advantage of being highly regulated.

Table 1. Clinical features[a]

Parameter	Ketamine+ (n = 20)	Ketamine− (n = 20)	P
Age (yr)	39 (32 to 50)	42 (32 to 50)	0.95
BMI (kg/m²)	22.5 (20.6 to 26.2)	22.3 (20.5 to 26.2)	0.89
Baseline creatininemia (μmol/L)	61.0 (56.8 to 64.2)	59.5 (52.0 to 64.0)	0.86
MDRD eGFR (ml/min per 1.73 m²)	100 (95 to 117)	107 (89 to 125)	0.79
H0 MAP (mmHg)	97 (88 to 103)	93 (80 to 110)	0.37
H1 MAP (mmHg)	83 (73 to 90)	83 (72 to 93)	0.97
H0 U_{Alb}/U_{Creat} (mg/mmol)	0.8 (0.5 to 1.3)	0.7 (0.5 to 1.5)	0.64

[a]Characteristics of patients, according to the use of ketamine. Data are median (25th to 75th percentiles). Values in Ketamine+ and Ketamine− groups are compared by Mann-Whitney U test. eGFR, estimated GFR; MAP, mean arterial pressure.

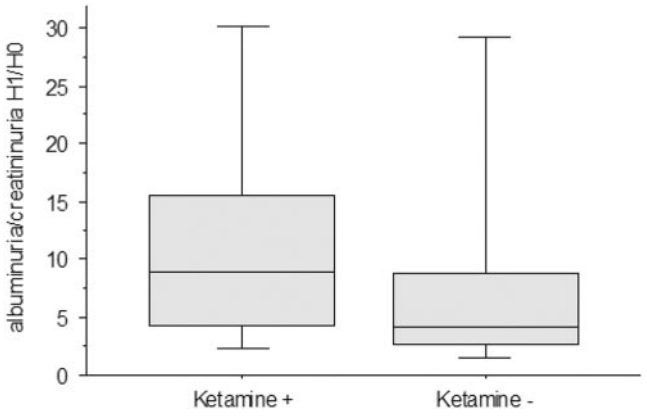

Figure 8. Effects of ketamine administration during general anesthesia. The graph illustrates the change after anesthesia (H1/H0) of the U_{Alb}/U_{Creat} values (mg/mmol) in patients who received ketamine (ketamine+) compared with those who did not (ketamine−). The horizontal lines inside the boxes represent median values, whereas bottom and top edges of the boxes represent the 25th and 75th percentiles and bottom and top whiskers reach the 10th and 90th percentiles, respectively.

Processes of highly regulated exocytosis involve a complex interplay among numerous proteins that coordinate vesicle transport, docking, priming, fusion, and recycling events, most of them subjected to fine modulation. Among modulating factors, one of the best studied is Rab3A, a versatile catalyst that tightly controls vesicle release probability.[33]

In neurons, Rab3A is an important late element in the establishment of the mature characteristics of presynaptic terminals.[18] Rab3A is also considered a marker of maturation in cultured pancreatic rudiments[34]; therefore, its appearance in mature glomeruli is coherent with these data and is compatible with our hypothesis of the usefulness of neuron-like signaling to cope with postnatal microenvironmental changes. The absence of glutamate release in undifferentiated podocytes and its appearance in differentiated cells further prove that a developed synaptic-like transmission is a property of mature podocytes.

Absence of Rab3A from KO glomeruli manifests itself with a relatively mild renal phenotype, witnessed by steady macroalbuminuria, which is in keeping with the very mild neurologic phenotype of these animals.[35] but, different from neurons, where synapse morphology looks intact,[36] podocytes display alterations detectable by transmission electron microscopy and scanning electron microscopy. Immunofluorescence integrates these findings, showing focal segmental decrease of podocyte proteins and providing molecular support to the evidence of macroalbuminuria. From these data, we can therefore argue that a tight modulation of glutamate exocytosis, such as the one performed by Rab3A, may be required for the correct functioning of the filtration barrier.

Our *in vitro* studies seem to help in understanding the type of alteration determined by Rab3A absence. Different from WT cells, Rab3A-KO podocytes display a sustained spontaneous exocytosis that impairs correct answers when a stimulus is applied. Here, previous data on neurotransmitter release by cells obtained from Rab3A-null mice concordantly show changes in vesicle transport and fusion, suggesting that Rab3A plays a role in controlling the number of available vesicles in an activity-dependent way.[37]

In KO podocytes, the dysregulated pattern of signaling could be explained by the concomitant reduction of two Rab3A effectors: Rabphilin-3A and Synapsin-I. A decreased rabphilin-3A has been repeatedly documented in Rab3A-KO mice, and a series of experiments have demonstrated that, in absence of Rab3A, rabphilin-3A becomes unstable and is degraded.[38] Here we show that in Rab3A-KO podocytes, there is also a decrease of Synapsin-I. Both rabphilin-3A and Synapsin-I are important regulators of the binding of vesicles to actin,[23,24] and their reduction can likely account for increased freedom of vesicles to be spontaneously released. Our data on the relative prevalence of phospho-Synapsin-I in KO cells points in the same direction, because Synapsin-I phosphorylation is a precise signal to release vesicles from actin.[39]

At the synapse, actin is the most prominent cytoskeletal protein.[26] Notably, in both neurons and podocytes, actin is highly enriched in the tiny projections that depart from major processes, namely dendritic spines and foot processes,[9] and actin dynamics have been proved essential for maintaining and regulating these specialized compartments.[26,40]

Our data show profound cytoskeletal changes in podocytes after *in vitro* NMDAR blockade. In neuronal cells, NMDARs are intimately associated with the actin cytoskeleton. Indeed, actin is directly coupled to the NMDAR *via* α-actinin and spectrin.[41,42] Interdependence between NMDAR activity and integrity of the actin cytoskeleton has been demonstrated; influx of extracellular calcium *via* NMDAR activation causes stabilization of actin,[43] whereas excessive NMDAR activation or blockade induces actin depolymerization,[44] and actin depolymerization strongly affects NMDAR activity.[45]

As for the consensual myosin-IIA redistribution observed in our experiments, it is known that nonmuscle myosin-IIA is present in foot processes,[40] although few studies have addressed its role. Myosin-IIA mutations are causative of Fetchner syndrome, whose renal phenotype is characterized by proteinuria and segmental foot process effacement.[46] Myosin-IIA is also expressed postsynaptically by mature neurons, where it has a role in structural plasticity of excitatory synapses.[47] Interestingly, a proteomic analysis has identified nonmuscle myosin as a component of the complex of proteins associated with the NMDAR.[48]

At the synapse, NMDAR-effected postsynaptic calcium rise activates CaMKII, which acts on downstream molecules, such as cofilin, influencing actin dynamics that regulate activity-dependent changes in synaptic strength.[49] This pathway seems operative also in podocytes, where actin reorganization after NMDAR antagonists appears secondary to reduced phosphorylation of CaMKII and cofilin, likely consequent to reduced calcium entry as a result of closure of the NMDAR channel. It

was shown that the very same pathway plays an important role in dendritic spine remodeling and specifically requires NMDAR, because analogue experiments performed on AMPA receptors do not have the same effects.[50]

The specificity of effects caused by NMDAR blockers and the similarity of events occurring in podocytes and neurons seem further proved by their reversibility after addition of the specific agonist NMDA and by the rebound NMDAR increase. This NMDAR increase is so rapid that it can be achieved only by trafficking of the receptor itself along the cytoskeleton; at least in neurons, actin remodeling is thought to serve exactly to this purpose.[51]

Together with these features, podocytes specifically displayed disappearance of nephrin from podocyte processes, a variation that prompted our subsequent experiments on isolated glomeruli and *in vivo*. Changes in nephrin expression have been shown to accompany or even precede most forms of experimental and human proteinuric diseases,[52] and, indeed, nephrin changes were the only podocyte alterations accompanying the increased albuminuria in norketamine-treated animals. Although the extremely low dosage and duration of norketamine treatment *in vivo* guarantee the absence of major neurologic consequences and stand for the action of norketamine on the glomerulus, the experiments performed on isolated glomeruli are those providing evidence of the direct effect of NMDAR antagonists on glomerular filtration. The usefulness of the method has been repeatedly proved in different experimental settings.[53,54] In this work it even confirmed the predicted stronger, less reversible action of MK-801.

In summary, our data seem to provide evidence in favor of the hypothesis that glutamatergic signaling driven by podocytes is relevant to the integrity of the filtering barrier, because its derangements are accompanied by podocyte changes and increased albuminuria. Analogue results have been shown in other cells, such as osteoblasts, in which NMDAR antagonists inhibit differentiation and matrix mineralization,[55] leading us to speculate that highly specialized cells, requiring continuous modulation of their activity, rely on the spatial and temporal precision of glutamate to finely tune their most regulated functions. Although preliminary and conducted on a limited number of cases, the human study adds to our observations an initial evidence of the potential importance of this system in the clinical setting and certainly suggests the usefulness of further investigation in this direction.

CONCISE METHODS

Animal Models

All rodent protocols strictly adhered to the Public Health Service Policy on Humane Care and Use of Laboratory Animals, and were approved by the Milan University Institutional Care and Ethical Treatment Committee. All animals were housed on a 12-h light/dark cycle, and allowed free access to food and water.

Balb/c mice and homozygous *H-2K^b*-tsA58 transgenic mice were acquired from Charles River Laboratories Italia (Calco, Lecco, Italy). Sprague-Dawley rats were from Harlan (S. Pietro al Natisone, Udine, Italy).

Rab3A KO mice (Rab3A-KO; Rab3A−/−; B6;129S-*Rab3a^{tm1Sud}*/J) and the appropriate WT (Rab3A-WT, Rab3A+/+; B6129SF2/J) were from Jackson Laboratory (Bar Harbor, ME). Backcrosses were generated, and the offspring were genotyped using the following primers: KO forward GCC GCA CGG AGA GGA AGA ATA GG; KO reverse CGG TGG GCT CTA TGG CTT CTG A (amplification product 900 bp); WT forward GCG CAA CCC AGG TCC ACA CA; WT reverse ACG CAC AAG CCT CCC GCA AG (amplification product 210 bp). Genotyping of the *H-2K^b*-tsA58 transgenic was conducted by the following primers: forward GTC ACA CCA CAG AAG TAA GGT TCC; reverse AGC GCT TGT GTC GCC ATT GTA TTC.

Podocyte Cell Cultures

For primary cultures, kidneys were taken from 7- to 10-d-old rodents, as described previously.[17] Briefly, glomeruli were isolated by sieving, then seeded in culture flasks (Corning, Sigma-Aldrich, Milan, Italy) precoated with collagen type IV (Sigma-Aldrich) at 37°C in 5% CO_2 atmosphere. After 1 wk, first-passage podocytes were separated from glomeruli by an additional sieving through the 36-μm mesh. Second-passage podocytes were seeded on flasks and thermanox coverslips (Nunc, VWR Int., Milan, Italy). Cell characterization was performed by morphology and immunofluorescence, using podocyte (nephrin, podocin), epithelial (cytokeratins), smooth muscle (α-smooth muscle actin), and endothelial cell (CD31) markers.

For the conditionally immortalized cell line, we followed with minor modifications the procedure originally published by Mundel *et al.*[19] Briefly, glomeruli were isolated from kidneys of adult (10-wk-old) transgenic *H-2K^b*-tsA58 mice by the same procedure as described already and grown first in standard medium at 37°C. Second-passage cells were replated and propagated at 33°C in medium containing 20 U/ml recombinant mouse γ-IFN (Sigma-Aldrich). Limiting dilution (10.0, 1.0, and 0.1 cells/vial) of these cells was followed by characterization, and only five clones expressing WT1 and nephrin on >90% of cells were selected and propagated. For initiation of differentiation, cells were thermo-shifted to 37°C and maintained in medium without γ-IFN.

Spontaneous and Stimulated Glutamate Release Assay

As described previously,[17,56] glutamate release was detected by an enzymatic assay based on the following reaction that occurs in the presence of glutamate dehydrogenase: $Glutamate^- + NAD^+ + H_2O \leftrightarrow ketoglutarate^{2-} + NADH + NAD^{4+} + H^+$ (all reagents from Sigma-Aldrich).

In brief, podocytes were plated and grown to semiconfluence. Before measurements, cells were thoroughly washed and incubated for 1 h at 37°C in DMEM-F12 buffer containing 1 mM $MgCl_2$ and 20 mM HEPES. The medium was further supplemented with glutamate dehydrogenase (60 U/ml) and NAD^+ (1 mM) and incubated for 5 min. Then, either medium (to evaluate spontaneous exocytosis) or 2.5 nM α-LTX was added, and spectrophotometric increase of OD due to increase of NADH was monitored at 340 nm every 10 min. Results were expressed as percentage variations from the baseline.

In Vivo Monitoring of Recycling Vesicles

The styryl dye FM1–43 (Invitrogen, S. Giuliano Milanese, Italy), which has no fluorescence properties in aqueous solution but becomes fluorescent on membrane binding, allows the labeling of recycling vesicles that is easily detectable by fluorescence microscopy.[57] In our experiments, the dye was added to the cell medium at a 2-μM concentration. Cells were maintained under observation for the whole duration of the experiment by the AxioVert 40 microscope (Zeiss, Arese, Mi, Italy) equipped for immunofluorescence. Dye fluorescence (wave length excitation 479; emission 598) of cells incubated in medium and after addition of 2.5 nM α-LTX was recorded by a digital videocamera (AxioCam MRC; Zeiss), with acquisition parameters settled by the "*live*" module of the software AxioVision (Zeiss).

Animal Studies

See supplemental material.

Immunofluorescence Studies

See supplemental material.

Immunogold Electron Microscopy

An indirect immunogold labeling procedure was performed on ultrathin frozen kidney sections, as described previously.[16] Briefly, after blocking, the material was incubated with the primary antibody followed by the proper secondary gold-conjugated goat anti-rabbit or goat anti-mouse IgG (H+L) 12 nm (Jackson ImmunoResearch Europe, Suffolk, UK).

Specificity of antibody labeling was demonstrated by the lack of staining after substituting proper control Igs (Invitrogen) for the primary antibody.

Western Blot

See supplemental material.

Convective Glomerular PAlb Test

As described previously,[58] Sprague-Dawley rat glomeruli were isolated by sieving from the renal cortex in isotonic PBS, and 5 g/dl BSA was added to the medium as an oncotic agent. Glomeruli were videotaped through an inverted microscope before and after the medium exchange from 5 to 1 g/dl BSA, used to create an oncotic gradient across the basement membrane, that resulted in a measurable glomerular volume change [$\Delta V = (V_{final} - V_{initial})/V_{initial}$], which could be measured off-line by a video-based image analysis software (Sigma Scan Pro) that determines the area of the glomerulus in the two-dimensional space and calculates the volume by a mathematical formula.

Because there is a direct relationship between the increase in glomerular volume (ΔV) and the oncotic gradient ($\Delta\Pi$) applied across the capillary wall, this principle was applied to calculate σalb, using the ratio of ΔV of experimental to ΔV of control glomeruli in response to identical oncotic gradients: $\sigma alb = \Delta V_{experimental}/\Delta V_{control}$. Convectional PAlb was therefore defined as $(1 - \sigma alb)$ to describe the movement of albumin consequent to water flow. When σalb is 0, albumin moves at the same rate as water and PAlb is 1.0. Alternatively, when σalb is 1.0, albumin cannot cross the membrane with water and PAlb is 0. It is assumed that the experiment is positive to PAlb test when values are $\geq$0.5.

NMDAR Blockade

The glutamate receptor antagonist norketamine hydrochloride (Tocris Bioscience, Bristol, UK) was diluted into the cell medium at the concentration of 50 μM for 30 min, whereas the more potent antagonist MK801 (Tocris Bioscience) was added at a concentration of 10 μM. In some experiments, the agonist NMDA (Tocris Bioscience) was added at a concentration of 50 μM for 15 min.

Human Study

The human study design was in accordance to the Declaration of Helsinki. After informed consent to the study, consecutive patients scheduled for gynecologic surgery were prospectively included during a period of 2 mo. All patients were orally premedicated with 1.5 mg/kg hydroxyzine, then randomly assigned to receive intraoperative low-dosage chlorhydrate ketamine (intravenous bolus of 0.15 mg/kg; ketamine+ group) for preemptive analgesic effect or nothing (ketamine− group), during standardized induction of general anesthesia (0.3 μg/kg sufentanyl, 2 to 3 mg/kg propofol, and 0.5 mg/kg atracrium, followed by maintenance with 6 to 9 mg/kg propofol or 1.0 to 1.5% isoflurane in 50% N_2O/40% O_2). Both protocols were routinely in use.

Inclusion criteria were age (20 to 60 yr) and admittance for celioscopic or transvaginal surgery. Patients presenting preexisting stages 3 through 5 chronic kidney disease (estimated GFR using the four-variable Modification of Diet in Renal Disease [MDRD] study equation $<$60 ml/min per 1.73 m^2), baseline $U_{Alb}/U_{Creat} > 3.39$ mg/mmol, diabetes, renin-angiotensin-aldosterone blocker medication, or preexisting allergy to ketamine were not included in the study.

Exclusion criteria were the use of hydroxyethyl starch and per-procedure hemodynamic instability (defined by fluid loading $>$1000 ml crystalloid/30 min and/or use of vasopressors). Data included patients' age and body mass index. Surgical route, type and volume of fluid infusion, drugs used for anesthesia maintenance, and antibiotic prophylaxis regimen were additionally collected. Noninvasive mean arterial pressure was measured before (H0) and 1 h after (H1) ketamine administration. U_{Alb} (immunonephelometry, Dade Behring BNII) and U_{Creat} (colorimetric Jaffé method, Beckman CX) were measured on urine samples collected by urinary catheterization at H0 and H1, before any postoperative analgesic medication was given.

Primary objective of this pilot study was to compare U_{Alb}/U_{Creat} difference between H0 and H1 in ketamine+ and ketamine− groups. Descriptive analyses were performed using median values (25th to 75th percentiles) for continuous variables and percentages for categorical variables. Values were compared with Mann-Whitney *U* test or Fisher exact test, as appropriate.

ACKNOWLEDGMENTS

We thank Guido Brusini for technical assistance and Vincent Compere, MD, PhD, and Sophie Claeyssens, MD, for contribution to the human study.

DISCLOSURES

None.

REFERENCES

1. Tryggvason K, Patrakka J, Wartiovaara J: Hereditary proteinuria syndromes and mechanisms of proteinuria. *N Engl J Med* 354: 1387–1401, 2006
2. Putaala H, Soininen R, Kilpelainen P, Wartiovaara J, Tryggvason K: The murine nephrin gene is specifically expressed in kidney, brain and pancreas: Inactivation of the gene leads to massive proteinuria and neonatal death. *Hum Mol Genet* 10: 1–8, 2001
3. Donoviel DB, Freed DD, Vogel H, Potter DG, Hawkins E, Barrish JP, Mathur BN, Turner CA, Geske R, Montgomery CA, Starbuck M, Brandt M, Gupta A, Ramirez-Solis R, Zambrowicz BP, Powell DR: Proteinuria and perinatal lethality in mice lacking NEPH1, a novel protein with homology to NEPHRIN. *Mol Cell Biol* 21: 4829–4836, 2001
4. Ciani L, Patel A, Allen ND, ffrench-Constant C: Mice lacking the giant protocadherin mFAT1 exhibit renal slit junction abnormalities and a partially penetrant cyclopia and anophthalmia phenotype. *Mol Cell Biol* 23: 3575–3582, 2003
5. Roselli S, Heidet L, Sich M, Henger A, Kretzler M, Gubler MC, Antignac C: Early glomerular filtration defect and severe renal disease in podocin-deficient mice. *Mol Cell Biol* 24: 550–560, 2004
6. Shih NY, Li J, Karpitskii V, Nguyen A, Dustin ML, Kanagawa O, Miner JH, Shaw AS: Congenital nephrotic syndrome in mice lacking CD2-associated protein. *Science* 286: 312–315, 1999
7. Kos CH, Le TC, Sinha S, Henderson JM, Kim SH, Sugimoto H, Kalluri R, Gerszten RE, Pollak MR: Mice deficient in alpha-actinin-4 have severe glomerular disease. *J Clin Invest* 111: 1683–1690, 2003
8. Reiser J, Polu KR, Möller CC, Kenlan P, Altintas MM, Wei C, Faul C, Herbert S, Villegas I, Avila-Casado C, McGee M, Sugimoto H, Brown D, Kalluri R, Mundel P, Smith PL, Clapham DE, Pollak MR: TRPC6 is a glomerular slit diaphragm-associated channel required for normal renal function. *Nat Genet* 37: 739–744, 2005
9. Kobayashi N, Gao SY, Chen J, Saito K, Miyawaki K, Li CY, Pan L, Saito S, Terashita T, Matsuda S: Process formation of the renal glomerular podocyte: Is there common molecular machinery for processes of podocytes and neurons? *Anat Sci Int* 79: 1–10, 2004
10. Gerke P, Benzing T, Höhne M, Kispert A, Frotscher M, Walz G, Kretz O: Neuronal expression and interaction with the synaptic protein CASK suggest a role for Neph1 and Neph2 in synaptogenesis. *J Comp Neurol* 498: 466–475, 2006
11. Beltran PJ, Bixby JL, Masters BA: Expression of PTPRO during mouse development suggests involvement in axonogenesis and differentiation of NT-3 and NGF-dependent neurons. *J Comp Neurol* 456: 384–395, 2003
12. Gloy J, Reitinger S, Fischer KG, Schreiber R, Boucherot A, Kunzelmann K, Mundel P, Pavenstadt H: Amino acid transport in podocytes. *Am J Physiol Renal Physiol* 278: F999–F1005, 2000
13. Mundel P, Heid HW, Mundel TM, Kruger M, Reiser J, Kritz W: Synaptopodin: An actin-associated protein in telencephalic dendrites and renal podocytes. *J Cell Biol* 139: 193–204, 1997
14. Peitsch WK, Hofmann I, Endlich N, Pratzel S, Kuhn C, Spring H, Grone HJ, Kriz W, Franke WW: Cell biological and biochemical characterization of drebrin complexes in mesangial cells and podocytes of renal glomeruli. *J Am Soc Nephrol* 14: 1452–1463, 2003
15. Cohen CD, Doran PP, Blattner SM, Merkle M, Wang GQ, Schmid H, Mathieson PW, Saleem MA, Henger A, Rastaldi MP, Kretzler M: Sam68-like mammalian protein 2, identified by digital differential display as expressed by podocytes, is induced in proteinuria and involved in splice site selection of vascular endothelial growth factor. *J Am Soc Nephrol* 16: 1958–1965, 2005
16. Rastaldi MP, Armelloni S, Berra S, Li M, Pesaresi M, Poczewski H, Langer B, Kerjaschki D, Henger A, Blattner SM, Kretzler M, Wanke R, D'Amico G: Glomerular podocytes possess the synaptic vesicle molecule Rab3A and its specific effector rabphilin-3a. *Am J Pathol* 163: 889–899, 2003
17. Rastaldi MP, Armelloni S, Berra S, Calvaresi N, Corbelli A, Giardino LA, Li M, Wang GQ, Fornasieri A, Villa A, Heikkila E, Soliymani R, Boucherot A, Cohen CD, Kretzler M, Nitsche A, Ripamonti M, Malgaroli A, Pesaresi M, Forloni GL, Schlöndorff D, Holthofer H, D'Amico G: Glomerular podocytes contain neuron-like functional synaptic vesicles. *FASEB J* 20: 976–978, 2006
18. Stettler O, Moya KL, Zahraoui A, Tavitian B: Developmental changes in the localization of the synaptic vesicle protein rab3A in rat brain. *Neuroscience* 62: 587–600, 1994
19. Mundel P, Reiser J, Zúñiga Mejía Borja A, Pavenstädt H, Davidson GR, Kriz W, Zeller R: Rearrangements of the cytoskeleton and cell contacts induce process formation during differentiation of conditionally immortalized mouse podocyte cell lines. *Exp Cell Res* 236: 248–258, 1997
20. Sara Y, Virmani T, Deàk F, Liu X, Kavalali ET: An isolated pool of vesicles recycles at rest and drives spontaneous neurotransmission. *Neuron* 45: 563–573, 2005
21. Saviane C, Silver RA: Fast vesicle reloading and a large pool sustain high bandwidth transmission at a central synapse. *Nature* 439: 983–987, 2006
22. Südhof TC: Alpha-latrotoxin and its receptors: Neurexins and CIRL/latrophilins. *Annu Rev Neurosci* 24: 933–962, 2001
23. Baldini G, Martelli AM, Tabellini G, Horn C, Machaca K, Narducci P, Baldini G: Rabphilin localizes with the cell actin cytoskeleton and stimulates association of granules with F-actin cross-linked by alpha-actinin. *J Biol Chem* 280: 34974–34984, 2005
24. Ceccaldi PE, Grohovaz F, Benfenati F, Chieregatti E, Greengard P, Valtorta F: Dephosphorylated synapsin I anchors synaptic vesicles to actin cytoskeleton: An analysis by videomicroscopy. *J Cell Biol* 128: 905–912, 1995
25. Rao A, Craig AM: Activity regulates the synaptic localization of the NMDA receptor in hippocampal neurons. *Neuron* 19: 801–812, 1997
26. Cingolani LA, Goda Y: Actin in action: The interplay between the actin cytoskeleton and synaptic efficacy. *Nat Rev Neurosci* 9: 344–356, 2008
27. Xu Q, Ming Z, Dart AM, Du XJ: Optimizing dosage of ketamine and xylazine in murine echocardiography. *Clin Exp Pharmacol Physiol* 34: 499–507, 2007
28. Galici R, Boggs JD, Miller KL, Bonaventure P, Atack JR: Effects of SB-269970, a 5-HT7 receptor antagonist, in mouse models predictive of antipsychotic-like activity. *Behav Pharmacol* 19: 153–159, 2008
29. Flavell SW, Greenberg ME: Signaling mechanisms linking neuronal activity to gene expression and plasticity of the nervous system. *Annu Rev Neurosci* 31: 563–590, 2008
30. Genever PG, Skerry TM: Regulation of spontaneous glutamate release activity in osteoblastic cells and its role in differentiation and survival: Evidence for intrinsic glutamatergic signaling in bone. *FASEB J* 15: 1586–1588, 2001
31. Moriyama Y, Hayashi M: Glutamate-mediated signaling in the islets of Langerhans: A thread entangled. *Trends Pharmacol Sci* 24: 511–517, 2003
32. Hitchcock IS, Skerry TM, Howard MR, Genever PG: NMDA receptor-mediated regulation of human megakaryocytopoiesis. *Blood* 102: 1254–1259, 2003
33. Schlüter OM, Basu J, Südhof TC, Rosenmund C: Rab3 superprimes synaptic vesicles for release: Implications for short-term synaptic plasticity. *J Neurosci* 26: 1239–1246, 2006
34. Miralles F, Serup P, Cluzeaud F, Vandewalle A, Czernichow P, Scharf-

mann R: Characterization of beta cells developed in vitro from rat embryonic pancreatic epithelium. *Dev Dyn* 214: 116–126, 1999
35. Geppert M, Bolshakov VY, Siegelbaum SA, Takei K, De Camilli P, Hammer RE, Südhof TC: The role of Rab3A in neurotransmitter release. *Nature* 369: 493–497, 1994
36. Leenders AG, Lopes da Silva FH, Ghijsen WE, Verhage M: Rab3a is involved in transport of synaptic vesicles to the active zone in mouse brain nerve terminals. *Mol Biol Cell* 12: 3095–3102, 2001
37. Wang X, Thiagarajan R, Wang Q, Tewolde T, Rich MM, Engisch KL: Regulation of quantal shape by Rab3A: Evidence for a fusion pore-dependent mechanism. *J Physiol* 586: 3949–3962, 2008
38. Yang S, Farias M, Kapfhamer D, Tobias J, Grant G, Abel T, Bucan M: Biochemical, molecular and behavioral phenotypes of Rab3A mutations in the mouse. *Genes Brain Behav* 6: 77–96, 2007
39. Bähler M, Greengard P: Synapsin I bundles F-actin in a phosphorylation-dependent manner. *Nature* 326: 704–707, 1987
40. Faul C, Asanuma K, Yanagida-Asanuma E, Kim K, Mundel P: Actin up: Regulation of podocyte structure and function by components of the actin cytoskeleton. *Trends Cell Biol* 17: 428–437, 2007
41. Wyszynski M, Lin J, Rao A, Nigh E, Beggs AH, Craig AM, Sheng M: Competitive binding of alpha-actinin and calmodulin to the NMDA receptor. *Nature* 385: 439–442, 1997
42. Wechsler A, Teichberg VI: Brain spectrin binding to the NMDA receptor is regulated by phosphorylation, calcium and calmodulin. *EMBO J* 17: 3931–3939, 1998
43. Star EN, Kwiatkowski DJ, Murthy VN: Rapid turnover of actin in dendritic spines and its regulation by activity. *Nat Neurosci* 5: 239–246, 2002
44. Rosenmund C, Westbrook GL: Rundown of N-methyl-D-aspartate channels during whole-cell recording in rat hippocampal neurons: Role of Ca2+ and ATP. *J Physiol* 470: 705–729, 1993
45. Sattler R, Xiong Z, Lu WY, MacDonald JF, Tymianski M: Distinct roles of synaptic and extrasynaptic NMDAR in excitotoxicity. *J Neurosci* 20: 22–33, 2000
46. Ghiggeri GM, Caridi G, Magrini U, Sessa A, Savoia A, Seri M, Pecci A, Romagnoli R, Gangarossa S, Noris P, Sartore S, Necchi V, Ravazzolo R, Balduini CL: Genetics, clinical and pathological features of glomerulonephritis associated with mutations of nonmuscle myosin IIA (Fechtner syndrome). *Am J Kidney Dis* 41: 95–104, 2003
47. Fifkova E, Morales M: Calcium-regulated contractile and cytoskeletal proteins in dendritic spines may control synaptic plasticity. *Ann N Y Acad Sci* 568: 131–137, 1989
48. Husi H, Ward MA, Choudhary JS, Blackstock WP, Grant SG: Proteomic analysis of NMDA receptor-adhesion protein signaling complexes. *Nat Neurosci* 3: 661–669, 2000
49. Bliss TV, Collingridge GL: A synaptic model of memory: Longterm potentiation in the hippocampus. *Nature* 361: 31–39, 1993
50. Thalhammer A, Rudhard Y, Tigaret CM, Volynski KE, Rusakov DA, Schoepfer R: CaMKII translocation requires local NMDA receptor-mediated Ca2+ signaling. *EMBO J* 25: 5873–5883, 2006
51. Fujisawa S, Shirao T, Aoki C: *In vivo*, competitive blockade of N-methyl-D-aspartate receptors induces rapid changes in filamentous actin and drebrin A distributions within dendritic spines of adult rat cortex. *Neuroscience* 140: 1177–1187, 2006
52. Holthöfer H: Molecular architecture of the glomerular slit diaphragm: Lessons learnt for a better understanding of disease pathogenesis. *Nephrol Dial Transplant* 22: 2124–2128, 2007
53. Candiano G, Musante L, Carraro M, Faccini L, Campanacci L, Zennaro C, Artero M, Ginevri F, Perfumo F, Gusmano R, Ghiggeri GM: Apolipoproteins prevent glomerular albumin permeability induced *in vitro* by serum from patients with focal segmental glomerulosclerosis. *J Am Soc Nephrol* 12: 143–150, 2001
54. Candido R, Carraro M, Fior F, Artero ML, Zennaro C, Burrell LM, Davis BJ, Cattin MR, Bardelli M, Faccini L, Carretta R, Fabris B: Glomerular permeability defect in hypertension is dependent on renin angiotensin system activation. *Am J Hypertens* 18: 844–850, 2005
55. Spencer GJ, McGrath CJ, Genever PG: Current perspectives on NMDA-type glutamate signaling in bone. *Int J Biochem Cell Biol* 39: 1089–1104, 2007
56. Bezzi P, Carmignoto G, Pasti L, Vesce S, Rossi D, Rizzini BL, Pozzan T, Volterra A: Prostaglandins stimulate calcium-dependent glutamate release in astrocytes. *Nature* 391: 281–285, 1998
57. Cousin MA, Robinson PJ: Mechanisms of synaptic vesicle recycling illuminated by fluorescent dyes. *J Neurochem* 73: 2227–2239, 1999
58. Savin VJ, Sharma R, Lovell HB, Welling DJ: Measurement of albumin reflection coefficient with isolated rat glomeruli. *J Am Soc Nephrol* 3: 1260–1269, 1992

See related editorial, "Signaling at the Slit: Podocytes Chat by Synaptic Transmission," on pages 1862–1864.

Supplemental information for this article is available online at http://www.jasn.org/.